

# Spinning test particles in the $\gamma$ space-time

Bobir Toshmatov<sup>1,2,\*</sup> and Daniele Malafarina<sup>1,†</sup>

<sup>1</sup>*Department of Physics, Nazarbayev University, 53 Kabanbay Batyr, 010000 Nur-Sultan, Kazakhstan*

<sup>2</sup>*Ulugh Beg Astronomical Institute, Astronomicheskaya 33, Tashkent 100052, Uzbekistan*

We consider the motion of spinning particles in the field of a well known vacuum static axially-symmetric space-time, known as  $\gamma$ -metric, that can be interpreted as a generalization of the Schwarzschild manifold to include prolate or oblate deformations. We derive the equations of motion for spinning test particles by using the Mathisson-Papapetrou-Dixon equations together with the Tulczyjew spin-supplementary condition, and restricting the motion to the equatorial plane. We determine the limit imposed by super-luminal velocity for the spin of the particle located at the innermost stable circular orbits (ISCO). We show that the particles on ISCO of the prolate  $\gamma$  space-time are allowed to have higher spin than the corresponding ones in the oblate case. We determine the value of the ISCO radius depending on the signature of the spin-angular momentum,  $s - L$  relation, and show that the value of the ISCO with respect to the non spinning case is bigger for  $sL < 0$  and smaller for  $sL > 0$ . The results may be relevant for determining the properties of accretion disks and constraining the allowed values of quadrupole moments of astrophysical black hole candidates.

## I. INTRODUCTION

Most of the current astrophysical observations of extreme compact objects such as black hole candidates, are obtained from light emitted by matter accreting around the compact object. It is natural to assume that matter in the accretion disks moves along geodesics and therefore from the study of geodesics we can infer useful information on the background geometry of the central object. In particular, circular orbits that are located close to the infinitely redshifted surface are extremely useful, as they provide information about the strong field regime and possibly the nature of the central object itself. Two of the most important circular orbits around compact objects are the light ring (photon sphere) and the innermost stable circular orbit (ISCO) for massive particles. In the static and spherically symmetric case, i.e. in the Schwarzschild case, the light ring and ISCO are located at  $r = 3M$  and  $r = 6M$ , respectively [1]. If the case of rotating black holes, i.e. in the Kerr case, the scenario is more complicated as locations of the characteristic orbits depend on the direction of the particle's orbital angular momentum ( $L$ ) and the spin of the central object ( $a$ ). More precisely, if the particle is co-rotating, i.e., moving in the rotation direction of the central object ( $aL > 0$ ), then the radii of the light ring and ISCO decrease with respect to the Schwarzschild case and at the extreme value of the rotation parameter ( $a = M$ ) they coincide at  $r = M$ . On the other hand, if the particle is counter-rotating, i.e., moving in the opposite rotation direction with respect to the central object ( $aL < 0$ ), then the radii of the light ring and ISCO increase with respect to the Schwarzschild case, and at the extreme value of the rotation parameter they become  $r = 4M$  and  $r = 9M$ , respectively [2–4]. Similar results are obtained in the Kerr-Newmann family of space-times if one includes charge [5].

The recent detection of gravitational waves by LIGO and VIRGO have confirmed that the black holes [6] and neutron

stars [7] in the coalescence of the binary system are spinning. Indeed, in these events the masses of the two objects in the binary system were comparable. However, there exist astrophysical scenarios where one component of the binary system has negligible mass,  $m$ , as compared to the companion with mass  $M$  (i.e. as  $m \ll M$ ), thus making the test particle approximation a valid tool to determine the characteristic orbit. Typically, the case of dust particles orbiting a stellar mass black hole and the case of a neutron star orbiting a supermassive black hole fit in the above description.

The motion of spinning test particle in non-homogeneous gravitational fields has been considered in several articles (see [8–11] and references therein). Most of these studies are restricted to the “pole-dipole” approximation where just monopole (mass) and dipole (rotational angular momentum, i.e., spin) are taken into account [12]. The equations of motion of such systems are described by the Mathisson-Papapetrou-Dixon (MPD) equations [13–15] with some spin-supplementary condition (SSC). The validity of the MPD equations in the limit of strong fields has been discussed in [16, 17]. The SSC serves as a reference point inside the spinning body whose evolution is described by the equations of motion. In the literature, several SSCs have been proposed, such as, Tulczyjew [18], Pirani [19], etc. – for details, see [11]. Similarly, the characteristic orbits of spinning particles in non-rotating and rotating axially symmetric space-times, are shifted inward or outward depending on signature of the spin of the particle, with respect to the non-spinning case [20–32].

In this paper, by using the “pole-dipole” approximation, we study the motion of spinning particles in the  $\gamma$ -metric. The  $\gamma$  metric, also known as Zipoy-Vorhees space-time, is an asymptotically flat, vacuum solution of Einstein's equations which belongs to the Weyl class of static, axially symmetric space-times [33, 34]. The  $\gamma$  metric is fully characterized by only two parameters: one,  $M$ , related to the mass of the source, and the other,  $\gamma$ , which can be called deformation parameter, related to the shape of the source. The metric is continuously linked to the Schwarzschild metric through the value of  $\gamma$ , as the spherically symmetric case is recovered for  $\gamma = 1$ . The cases  $0 < \gamma < 1$  and  $\gamma > 1$  represent sources with prolate and

\* bobir.toshmatov@nu.edu.kz

† daniele.malafarina@nu.edu.kz

oblate spheroidal deformations, respectively. It is important to stress that in these cases, i.e. for  $\gamma \neq 1$ , the line element does not represent a black hole [35–37], as the surface  $r = 2M$  becomes a true curvature singularity. The motion of test particles in the  $\gamma$  metric was considered in [38–43] and it was shown that the space-time can be considered as black hole “mimicker” and constitutes an excellent candidate to study possible astrophysical tests of black hole candidates.

The paper is organized as follows: in Sec. II, we present the general formalism for spinning particles in the “pole-dipole” approximation, i.e., MPD equations with Tulczyjew - SSC and, we derive the equations of motion for spinning particles in a generic space-time. In Sec. III we apply derived equations to the  $\gamma$ -metric and calculate the ISCO for spinning particles and compare it with the Schwarzschild case. Finally, in Sec. IV we summarize the results and discuss how they could be relevant for astrophysical observations of black hole candidates. Throughout the paper, we use natural units setting  $G = c = 1$ .

## II. DYNAMICS OF SPINNING PARTICLES

The equations of motion of spinning test particles are determined by the MPD equations, which can be given as [13–15]

$$\frac{Dp^\alpha}{d\lambda} = -\frac{1}{2}R_{\beta\delta\sigma}^\alpha u^\beta S^{\delta\sigma}, \quad (1)$$

$$\frac{DS^{\alpha\beta}}{d\lambda} = p^\alpha u^\beta - u^\alpha p^\beta, \quad (2)$$

where  $D/d\lambda$  is the covariant derivative along the particle’s trajectory ( $D/d\lambda \equiv u^\alpha \nabla_\alpha$ ),  $\lambda$  is the affine parameter,  $R_{\beta\delta\sigma}^\alpha$  is the Riemann tensor,  $p^\alpha$  and  $u^\alpha$  are the dynamical 4-momentum and kinematical 4-velocity of the particle, respectively, and  $S^{\alpha\beta}$  is the spin tensor. Notice that  $S^{\alpha\beta}$  is antisymmetric (i.e.  $S^{\alpha\beta} = -S^{\beta\alpha}$ ) and so it has only six independent components. Obviously, the spinning particle does not follow a geodesic trajectory because of the spin-curvature force  $R_{\beta\delta\sigma}^\alpha u^\beta S^{\delta\sigma}$ .

To solve equations (1) and (2), we need one extra condition. Therefore, in order to restrict the spin tensor to generate rotations only, we employ the so called “Tulczyjew supplementary condition” (SSC) [18] given by

$$S^{\alpha\beta} p_\alpha = 0. \quad (3)$$

Then, from the above SSC, it turns out that both the canonical momentum and the spin of the particle are conserved quantities as

$$p^\alpha p_\alpha = -m^2, \quad (4)$$

$$S^{\alpha\beta} S_{\alpha\beta} = 2S^2. \quad (5)$$

However, it is worth noticing that, despite the canonical momentum of the spinning particle being conserved, its squared velocity does not necessarily satisfy the normalization condition  $u_\alpha u^\alpha = -1$ , as the 4-vectors  $p^\alpha$  and  $u^\alpha$  are not always parallel. Furthermore, in addition to the SSC-dependent conserved quantities, there are the usual background-dependent

conserved quantities associated with the Killing vectors,  $\xi^\alpha$ , which can be expressed as

$$C_\xi = p^\alpha \xi_\alpha - \frac{1}{2} S^{\alpha\beta} \nabla_\beta \xi_\alpha. \quad (6)$$

Since the spin tensor is antisymmetric and the Christoffel symbols  $\Gamma_{\alpha\beta}^\nu$  are symmetric, it immediately follows that  $S^{\alpha\beta} \Gamma_{\alpha\beta}^\nu = 0$ , and consequently, the background-dependent conserved quantities via Killing vectors (6) can be written as

$$C_\xi = p^\alpha \xi_\alpha - \frac{1}{2} S^{\alpha\beta} \partial_\beta \xi_\alpha. \quad (7)$$

The line element of a generic stationary axially symmetric space-time is given by

$$ds^2 = g_{tt} dt^2 + g_{rr} dr^2 + 2g_{t\phi} dt d\phi + g_{\theta\theta} d\theta^2 + g_{\phi\phi} d\phi^2 \quad (8)$$

where the metric functions depend on the coordinates  $r$  and  $\theta$ . From the symmetry of the metric one can easily see that the line element (8) allows for two Killing vector fields, one related to time translations and one to rotations, as given by

$$\xi^\alpha = \delta_t^\alpha, \quad \xi^\alpha = \delta_\phi^\alpha. \quad (9)$$

The corresponding conserved quantities, i.e. energy and angular momentum, can be written as

$$E = -p_t + \frac{1}{2} g_{t\alpha,\beta} S^{\alpha\beta}, \quad (10)$$

$$L = p_\phi + \frac{1}{2} g_{\phi\alpha,\beta} S^{\alpha\beta}. \quad (11)$$

When considering astrophysical applications, such as accretion disks, it is sufficient to consider test particles moving on the equatorial plane,  $\theta = \pi/2$ . When restricted to the equatorial plane the metric functions depend only on the radial coordinate and  $p^\theta = 0$ . The number of independent components of the spin tensor is reduced to three since

$$S^{\theta\alpha} = 0, \quad (12)$$

and for the remaining components, from the Tulczyjew-SSC (3), one finds the following relations:

$$S^{t\phi} = -\frac{p_r}{p_\phi} S^{tr}, \quad (13)$$

$$S^{r\phi} = \frac{p_t}{p_\phi} S^{tr}. \quad (14)$$

From the normalization condition (4) one finds the radial momentum of the particle given by

$$p_r^2 = g_{rr} (-g^{tt} p_t^2 - g^{\phi\phi} p_\phi^2 - 2g^{t\phi} p_t p_\phi - m^2). \quad (15)$$

By using the relations (13), (14), and (15) from the spin conservation law (5), one finds the  $(t, r)$ -component of the spin tensor as

$$S^{tr} = \pm \frac{p_\phi S}{\sqrt{g_{rr} (g_{t\phi}^2 - g_{tt} g_{\phi\phi})}} \quad (16)$$

where  $\pm$  signs represent the direction of spin with respect to direction of  $p_\phi$ . In expression (16) we have written the spin

parameter  $S$  in terms of the the specific spin angular momentum of the particle  $s$  as  $S = ms$ . Finally, from the conservation of energy (10) and angular momentum (11), we find the  $t$  and  $\phi$  components of the four-momentum as

$$p_t = \frac{-E + s(AL + BE)}{1 - s^2D}, \quad (17)$$

$$p_\phi = \frac{L + s(BL + CE)}{1 - s^2D}. \quad (18)$$

with

$$\begin{aligned} A &= \frac{g'_{tt}}{2\sqrt{g_{rr}(g_{t\phi}^2 - g_{tt}g_{\phi\phi})}}, \\ B &= \frac{g'_{t\phi}}{2\sqrt{g_{rr}(g_{t\phi}^2 - g_{tt}g_{\phi\phi})}}, \\ C &= \frac{g'_{\phi\phi}}{2\sqrt{g_{rr}(g_{t\phi}^2 - g_{tt}g_{\phi\phi})}}, \\ D &= B^2 - AC = \frac{(g'_{t\phi})^2 - g'_{tt}g'_{\phi\phi}}{4g_{rr}(g_{t\phi}^2 - g_{tt}g_{\phi\phi})}, \end{aligned}$$

where prime denotes the partial derivative with respect to radial coordinate as  $f' \equiv \partial f / \partial r$ . The contravariant forms of the momenta are determined by  $p^\alpha = g^{\alpha\beta}p_\beta$ .

By substituting expressions (17) and (18) into the radial component of the four-momentum (15) one arrives at the expression

$$(p^r)^2 = \frac{\beta}{\alpha}(E - V_+)(E - V_-), \quad (19)$$

where the effective potentials  $V_\pm$  are given by

$$V_\pm = -\frac{\delta L}{\beta} \pm \sqrt{\frac{\delta^2 L^2}{\beta^2} + \frac{\rho - \sigma L^2}{\beta}}, \quad (20)$$

and

$$\begin{aligned} \alpha &= g_{rr} \left[ 1 - \frac{s^2 \left( (g'_{t\phi})^2 - g'_{tt}g'_{\phi\phi} \right)}{4g_{rr} \left( g_{t\phi}^2 - g_{tt}g_{\phi\phi} \right)} \right]^2, \\ \beta &= -g^{tt} + \frac{s \left( g^{tt}g'_{t\phi} + g^{t\phi}g'_{\phi\phi} \right)}{\sqrt{g_{rr}(g_{t\phi}^2 - g_{tt}g_{\phi\phi})}} - \frac{s^2 \left[ g^{tt}(g'_{t\phi})^2 + g'_{\phi\phi} \left( 2g^{t\phi}g'_{t\phi} + g^{\phi\phi}g'_{\phi\phi} \right) \right]}{4g_{rr} \left( g_{t\phi}^2 - g_{tt}g_{\phi\phi} \right)}, \\ \delta &= g^{t\phi} + \frac{s \left( g^{tt}g'_{tt} - g^{\phi\phi}g'_{\phi\phi} \right)}{2\sqrt{g_{rr}(g_{t\phi}^2 - g_{tt}g_{\phi\phi})}} - \frac{s^2 \left[ g'_{t\phi} \left( g^{tt}g'_{tt} + g^{t\phi}g'_{t\phi} \right) + g'_{\phi\phi} \left( g^{t\phi}g_{tt} + g^{\phi\phi}g'_{t\phi} \right) \right]}{4g_{rr} \left( g_{t\phi}^2 - g_{tt}g_{\phi\phi} \right)}, \\ \sigma &= -g^{\phi\phi} - \frac{s \left( g^{t\phi}g'_{tt} - g^{\phi\phi}g'_{t\phi} \right)}{\sqrt{g_{rr}(g_{t\phi}^2 - g_{tt}g_{\phi\phi})}} - \frac{s^2 \left[ g^{tt}(g'_{tt})^2 + g'_{t\phi} \left( 2g^{t\phi}g'_{tt} + g^{\phi\phi}g'_{t\phi} \right) \right]}{4g_{rr} \left( g_{t\phi}^2 - g_{tt}g_{\phi\phi} \right)}, \\ \rho &= m^2 \left[ 1 - \frac{s^2 \left( (g'_{t\phi})^2 - g'_{tt}g'_{\phi\phi} \right)}{4g_{rr} \left( g_{t\phi}^2 - g_{tt}g_{\phi\phi} \right)} \right]^2. \end{aligned}$$

One can see from (19) that in order to have  $(p^r)^2 \geq 0$ , the energy of the particle must satisfy one of the following

conditions:

$$E \in (-\infty, V_-], \quad (21)$$

$$E \in [V_+, \infty). \quad (22)$$

In the following, we will restrict our attention to the case of test particles with positive energy and thus will restrict the attention to the effective potential  $V_{\text{eff}} = V_+$ .

Let us focus on the characteristic circular orbits of the spinning test particle in the space-time described by the line element (8). It is well known that circular motion of particles moving in the central field is governed by the following conditions:

- (i) The radial velocity of the particle must vanish at the circular orbit. Namely

$$\frac{dr}{d\lambda} = 0, \quad \text{which implies } V_+ = E, \quad (23)$$

- (ii) The radial acceleration of the particle must vanish. Namely

$$\frac{d^2r}{d\lambda^2} = 0, \quad \text{which implies } \frac{dV_+}{dr} = 0. \quad (24)$$

However, these conditions do not in general guarantee that the circular orbits are stable. Stability of the orbit is provided by positivity of the second derivative of the effective potential with respect to radial coordinate as

$$\frac{d^2V_+}{d\lambda^2} \geq 0, \quad (25)$$

with the equality holding for the marginally stable orbits, corresponding to the smallest allowed value for stable circular orbits, namely the ISCO.

Before proceeding to the motion of spinning test particles in the  $\gamma$ -metric, there is one more important feature which appears due to the spin of the particle that should be considered. That is the super-luminal bound on the particle's motion. As it was mentioned before, the dynamical 4-momentum and kinematical 4-velocity of the spinning particle are not always parallel. Therefore, the normalization  $u_\alpha u^\alpha = -1$  does not hold while,  $p_\alpha p^\alpha = -m^2$  is satisfied. As the spinning particle approaches the center of the space-time, its 4-velocity increases and eventually, for certain values of the spin and radius some components of the 4-velocity may diverge as  $u_\alpha u^\alpha \rightarrow +\infty$ . Before this to happen, the particle's motion crosses the boundary between time-like and space-like trajectories. Of course, space-like (i.e. super-luminal) motion is physically meaningless, and the transition to  $u_\alpha u^\alpha > 0$  is not allowed for real particles. Therefore one must impose a further bound, called super-luminal bound, which is defined by the relation  $u_\alpha u^\alpha = 0$ .

Within the Tulczyjew-SSC (3), one can find the components of the 4-velocity  $u^\alpha$  from the following velocity-momentum relation [44]:

$$u^\alpha = \frac{\mu}{m^2} \left( p^\alpha + \frac{2S^{\alpha\beta} R_{\beta\delta\sigma\rho} p^\delta S^{\sigma\rho}}{4m^2 + R_{abcd} S^{ab} S^{cd}} \right), \quad (26)$$

where  $\mu$  is kinematical mass (or rest mass) of the particle and it is defined by  $u^\alpha p_\alpha = -\mu$ . Explicit analytical forms of components of the 4-velocity,  $u^\alpha$ , in a generic stationary space-time (8) are very long. However, in the static case (i.e.  $g_{t\phi} = 0$ ), for motion restricted to the equatorial plane, they reduce to

$$\begin{aligned} u^t &= p_t \left\{ g^{tt} + \frac{(S^{tr})^2}{X} \left[ \frac{p_r^2}{p_\phi^2} \left( \frac{B_1}{g_{rr}} + \frac{C_1}{g_{tt}} \right) - \frac{A_1}{g_{tt}} + \frac{B_1}{g_{\phi\phi}} \right] \right\}, \\ u^r &= p_r \left\{ g^{rr} + \frac{(S^{tr})^2}{X} \left[ -\frac{p_t^2}{p_\phi^2} \left( \frac{B_1}{g_{rr}} + \frac{C_1}{g_{tt}} \right) + \frac{A_1}{g_{rr}} + \frac{C_1}{g_{\phi\phi}} \right] \right\}, \\ u^\theta &= 0, \\ u^\phi &= p_\phi \left\{ g^{\phi\phi} + \frac{(S^{tr})^2}{X} \left[ \frac{p_t^2}{p_\phi^2} \left( \frac{A_1}{g_{tt}} - \frac{B_1}{g_{\phi\phi}} \right) + \frac{p_r^2}{p_\phi^2} \left( \frac{A_1}{g_{rr}} + \frac{C_1}{g_{\phi\phi}} \right) \right] \right\}, \end{aligned} \quad (27)$$

where

$$\begin{aligned} X &= 4m^2 + (S^{tr})^2 \left( -A_1 + \frac{p_t^2}{p_\phi^2} B_1 + \frac{p_r^2}{p_\phi^2} C_1 \right), \\ A_1 &= \frac{g'_{rr} g'_{tt}}{g_{rr}} + \frac{(g'_{tt})^2}{g_{tt}} - 2g''_{tt}, \\ B_1 &= \frac{g'_{rr} g'_{\phi\phi}}{g_{rr}} + \frac{(g'_{\phi\phi})^2}{g_{\phi\phi}} - 2g''_{\phi\phi}, \\ C_1 &= \frac{g'_{tt} g'_{\phi\phi}}{g_{rr}}. \end{aligned} \quad (28)$$

Since in this paper, we are mainly concerned with circular orbits for the spinning test particle, and in particular with the ISCO, let us explicitly evaluate the super-luminal limit of spinning particles on circular orbits. In the case of circular orbits, the relation  $u^\alpha u_\alpha = 0$  becomes:

$$\frac{g_{tt} g_{\phi\phi} p_t^2 p_\phi^2 (S^{tr})^4}{\left[ 4p_\phi^2 - (S^{tr})^2 (B_1 p_t^2 - A_1 p_\phi^2) \right]^2} \left( \frac{B_1}{g_{\phi\phi}} - \frac{A_1}{g_{tt}} \right)^2 = 1, \quad (29)$$

Notice that in (29) the momentum and spin tensors are func-

tions of the spin and therefore, given the non trivial dependence on  $s$ , equation (29) cannot be solved analytically, even in the simplest case that is the Schwarzschild space-time.

Alternatively, one can use the method developed in [45]. From the second of the MPD equations (2) and the Tulczyjew-SSC (3) one finds the following relations <sup>1</sup>:

$$\begin{aligned} \frac{DS^{tr}}{d\lambda} &= -\frac{p_\phi}{p_t} \frac{DS^{\phi r}}{d\lambda} - \frac{S^{\phi r}}{p_t} \frac{Dp_\phi}{d\lambda} + S^{\phi r} \frac{p_\phi}{p_t^2} \frac{Dp_t}{d\lambda} \\ &= p^t u^r - p^r, \end{aligned} \quad (30)$$

$$\begin{aligned} \frac{DS^{t\phi}}{d\lambda} &= \frac{p_r}{p_t} \frac{DS^{\phi r}}{d\lambda} + \frac{S^{\phi r}}{p_t} \frac{Dp_r}{d\lambda} - S^{\phi r} \frac{p_r}{p_t^2} \frac{Dp_t}{d\lambda} \\ &= p^t u^\phi - p^\phi, \end{aligned} \quad (31)$$

where

$$\frac{DS^{\phi r}}{d\lambda} = p^\phi u^r - u^\phi p^r, \quad (32)$$

$$S^{\phi r} = \mp \frac{p_t s}{\sqrt{g_{rr}(g_{t\phi}^2 - g_{tt}g_{\phi\phi})}}, \quad (33)$$

and from the first of the MPD equations (1), one can write the covariant derivatives of the components of the dynamical 4-momentum as

$$\frac{Dp_\alpha}{d\lambda} = -\frac{1}{2} R_{\alpha\beta\delta\sigma} u^\beta S^{\delta\sigma}. \quad (34)$$

By using the above relations, one can solve equations (30) and (31) with respect to  $u^r$  and  $u^\phi$ , simultaneously. Thus, for the particle to move always in the time-like region, we must impose the following condition:

$$\frac{u_\alpha u^\alpha}{(u^t)^2} = g_{tt} + g_{rr}(u^r)^2 + 2g_{t\phi}u^\phi + g_{\phi\phi}(u^\phi)^2 \leq 0, \quad (35)$$

with equality holding for the super-luminal bound. In the next section we will adapt the above formalism to a background space-time given by the  $\gamma$ -metric and determine how the particle's spin in this space-time affects the motion in comparison with the Schwarzschild and Kerr space-times.

### III. SPINNING PARTICLE IN THE $\gamma$ -METRIC

The  $\gamma$  space-time, is a static axially symmetric vacuum solution of Einstein's equations that is represented by the line element [33, 34]

$$\begin{aligned} ds^2 &= -f^\gamma dt^2 + f^{\gamma^2 - \gamma} g^{1-\gamma^2} \left( \frac{dr^2}{f} + r^2 d\theta^2 \right) + \\ &\quad + f^{1-\gamma} r^2 \sin^2 \theta d\phi^2, \end{aligned} \quad (36)$$

where

$$\begin{aligned} f(r) &= 1 - \frac{2M}{r}, \\ g(r, \theta) &= 1 - \frac{2M}{r} + \frac{M^2 \sin^2 \theta}{r^2}. \end{aligned} \quad (37)$$

The line-element depends on two parameters,  $M$ , related to the mass of the source and  $\gamma$ , related to its deformation from spherical symmetry. To understand the meaning of such parameters we may consider the asymptotic expansion in multipoles of the gravitational potential [46]. Then it is easy to see that the total mass of the source (i.e. the monopole moment) as measured by an observer at infinity is  $M_{\text{tot}} = M\gamma$  and the quadrupole moment is  $Q = M^3\gamma(1 - \gamma^2)/3$ . The striking difference between the case  $\gamma = 1$  (i.e. Schwarzschild) and the case with non vanishing quadrupole moment comes from the analysis of the Kretschmann scalar which shows that the surface  $r = 2M$  is a curvature singularity [47]. Therefore the space-time is geodesically incomplete with the radial coordinate limited to values  $r \in (2M, \infty)$ . One traditional interpretation of the  $\gamma$ -metric suggests that static compact objects must tend to become spherical as they become more compact to the limit that they must shed away all higher multipole moments as they cross the horizon at  $r = 2M$ . However, perfect spherical symmetry is a mathematical abstraction that is not expected to exist in the real world. Therefore, another possible interpretation of the  $\gamma$ -metric can be considered if we are to understand the singularity as a regime where classical relativistic description fails. Then, we may allow for the existence of exotic compact objects with non vanishing quadrupole moment and we can interpret the surface  $r = 2M$  as the boundary of such object. The region close to  $r = 2M$  would then need a theory of quantum-gravity to be described and its high red-shift (that tends to infinity in the classical limit) would make such objects look like black holes to distant observers. We now ask the question whether, in principle, we can be able to distinguish a black hole space-time from the  $\gamma$ -metric by observing the motion of spinning particles in accretion disks.

From (16) one can write  $(t, r)$  component of the spin tensor as

$$S^{tr} = \frac{sp_\phi}{r} \left(1 - \frac{2M}{r}\right)^{(1-\gamma)\gamma/2} \left(1 - \frac{M}{r}\right)^{-1+\gamma^2}, \quad (38)$$

Then, from (17) and (18) one can write the covariant momenta of the neutral spinning test particle corresponding to the  $t$  and  $\phi$  coordinates as

$$p_t = -\frac{E + sAL}{1 - s^2D}, \quad (39)$$

$$p_\phi = \frac{L + sCE}{1 - s^2D}, \quad (40)$$

<sup>1</sup> By following the gauge choices and invariant relations in [45], the notation  $\lambda = t$  is adopted.



where for the  $\gamma$ -metric we have

$$\begin{aligned} A &= - \left(1 - \frac{2M}{r}\right)^{(2-\gamma)(\gamma-1)/2} \left(1 - \frac{M}{r}\right)^{\gamma^2-1} \frac{M\gamma}{r^3}, \\ B &= 0, \\ C &= \left(1 - \frac{2M}{r}\right)^{-\gamma(\gamma+1)/2} \left(1 - \frac{M}{r}\right)^{\gamma^2-1} \frac{r - M\gamma - M}{r}, \\ D &= \left(1 - \frac{2M}{r}\right)^{(1-\gamma)\gamma-1} \left(1 - \frac{M}{r}\right)^{2(\gamma^2-1)} \frac{M\gamma(r - M\gamma - M)}{r^4}. \end{aligned} \quad L \rightarrow -L, \quad s \rightarrow -s, \quad (42)$$

The radial momentum of the particle becomes

$$(p^r)^2 = \left(1 - \frac{2M}{r}\right)^{1-\gamma^2} \left(1 - \frac{M}{r}\right)^{2(\gamma^2-1)} \times \left[ p_t^2 - \left(1 - \frac{2M}{r}\right)^{2\gamma-1} \frac{p_\phi^2}{r^2} - m^2 \left(1 - \frac{2M}{r}\right)^\gamma \right], \quad (41)$$

as  $p^r(s, L) = p^r(-s, -L)$ . By writing the radial momentum (41) in terms of  $p_t$  and  $p_\phi$ , one arrives at the expression (19) with the following notations:

$$\begin{aligned} \alpha &= \left(1 - \frac{2M}{r}\right)^{(\gamma-1)\gamma-1} \left(1 - \frac{M}{r}\right)^{2(1-\gamma^2)} \left[ -1 + s^2 \left(1 - \frac{2M}{r}\right)^{(1-\gamma)\gamma-1} \left(1 - \frac{M}{r}\right)^{2(\gamma^2-1)} \frac{M\gamma(r - M\gamma - M)}{r^4} \right]^2, \\ \beta &= \left(1 - \frac{2M}{r}\right)^{-\gamma} - s^2 \left(1 - \frac{2M}{r}\right)^{-\gamma^2-1} \left(1 - \frac{M}{r}\right)^{2(\gamma^2-1)} \frac{(r - M\gamma - M)^2}{r^4}, \\ \delta &= -s \left(1 - \frac{2M}{r}\right)^{-(\gamma-1)\gamma/2-1} \left(1 - \frac{M}{r}\right)^{\gamma^2-1} \frac{(r - 2M\gamma - M)}{r^3}, \\ \sigma &= - \left(1 - \frac{2M}{r}\right)^{\gamma-1} \frac{1}{r^2} + s^2 \left(1 - \frac{2M}{r}\right)^{-(\gamma-2)\gamma-2} \left(1 - \frac{M}{r}\right)^{2(\gamma^2-1)} \frac{M^2\gamma^2}{r^6}, \\ \rho &= -m^2 \left[ -1 + s^2 \left(1 - \frac{2M}{r}\right)^{(1-\gamma)\gamma-1} \left(1 - \frac{M}{r}\right)^{2(\gamma^2-1)} \frac{M\gamma(r - M\gamma - M)}{r^4} \right]^2, \end{aligned} \quad (43)$$

Now, by inserting the above parameters into the expression for the effective potential  $V_+$  given by (20), one can easily write explicitly the effective potential for the spinning particle in the  $\gamma$ -metric. Given the length of the expression for  $V_+$  it is more useful to graphically study the radial profiles for different values of the spin parameter  $s$  of the test particle in space-times corresponding to slightly oblate (i.e.  $\gamma > 1$ ), slightly prolate (i.e.  $\gamma < 1$ ) sources. The explicit form of  $V_+$  is given in the appendix A.

The effective potentials are given in Fig. 1 and, given the possibility that the deformation parameter of a static source may produce effects on test particles similar to rotation of the source, we compared with the effective potentials for the Kerr space-time. One can see from Fig. 1 that, depending on the values of spin and angular momentum of the particle, the effective potential possesses two local extrema: a maximum and a minimum that correspond to the unstable and stable circular orbits, respectively. The effect of the spin on the value of circular orbits can be seen from Fig. 1. As the spin of the particle increases, the radii of the both stable and unstable circular orbits decrease. Conversely, as the spin of the particle

decreases, the radii of the both stable and unstable circular orbits increase. Furthermore, similarly to what was obtained for non-spinning particles in [43], the  $\gamma$ -metric for an oblate spheroidal source has stable and unstable circular orbits with bigger radii for the test particles with respect to the  $\gamma$ -metric for a prolate spheroidal source.

It is well-known that one of the most important orbits around compact objects in astrophysics is the ISCO, which determines the inner edge of accretion disks. As we have seen the value of circular orbits is affected by the spin of the test particles and therefore the value of the ISCO is also subject to change depending on the spin of the particles in the disk. In the case of the  $\gamma$ -metric, the expression of the radial momentum of the spinning particle (41) is rather long and it can be found in the appendix A. Here we will restrict to numerical results that illustrate the dependence of the ISCO on the spin of the particles. However, before turning the attention to circular orbits, one must remember that for the particle's motion to be physically realistic, we need to determine the limits imposed by the super-luminal bound. To find the super-luminal limit, one needs to find the kinematical 4-velocity which was given

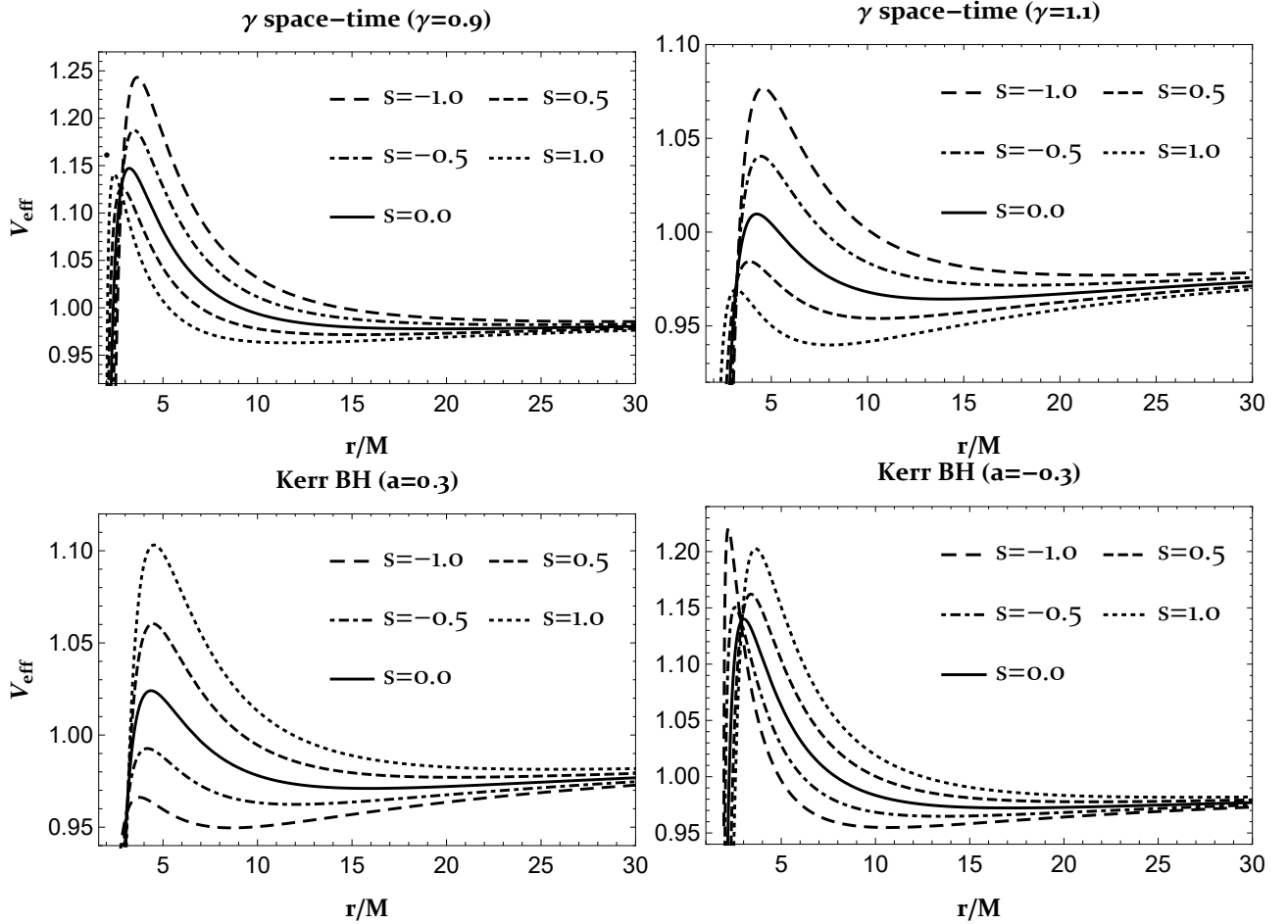


FIG. 1. Top panel: radial profile of the effective potentials of the spinning test particle in the  $\gamma$  space-time with prolate ( $\gamma = 0.9$ , left panel) and oblate ( $\gamma = 1.1$ , right panel) source for different values of the particle's spin. Bottom panel: radial profile of the effective potentials of co-rotating (left panel) and counter-rotating (right panel) spinning test particles in the Kerr black hole with different values of spin. In all plots, the specific angular momentum of the particle is fixed as  $L/m = 4.5$ .

in equations (27) for spinning particles in the equatorial plane.

The coefficients (28) in terms of the  $\gamma$  space-time become

$$\begin{aligned}
 A_1 &= \left(1 - \frac{M}{r}\right) \left(1 - \frac{2M}{r}\right)^{\gamma-2} \frac{4M\gamma [2r^2 - 2(\gamma+2)Mr + (\gamma+1)^2M^2]}{r^5}, \\
 B_1 &= -\left(1 - \frac{M}{r}\right) \left(1 - \frac{2M}{r}\right)^{-\gamma-1} \frac{4M\gamma [r^2 - (\gamma+2)Mr + \gamma(\gamma+1)M^2]}{r^3}, \\
 C_1 &= \left(1 - \frac{2M}{r}\right)^{(1-\gamma)\gamma} \left(1 - \frac{M}{r}\right)^{2\gamma^2-2} \frac{4M\gamma(r - M\gamma - M)}{r^2}.
 \end{aligned} \tag{44}$$

Now, by inserting expressions (38), (39), (40) and (44) into (29), one can find the super-luminal bound values of the spinning particle in the  $\gamma$  space-time. These values for a particle located on the ISCO are presented in Fig. 2 for different values of  $\gamma$ . Further, in Tab. I we relate the values of  $s(\max)$  in Fig. 2 to the values of the parameters characterizing the parti-

cle's motion at the ISCO. One can see from Tab. I and Fig. 2 that when the space-time has prolate deformation, the spinning particle at the ISCO is allowed to have higher value of spin relative to the ones in the not deformed and oblately deformed space-times. With a change of the deformation from prolate towards oblate, the limit of spin of the particle decreases quite rapidly till the value  $s(\max) \approx 1.58$  at the ISCO

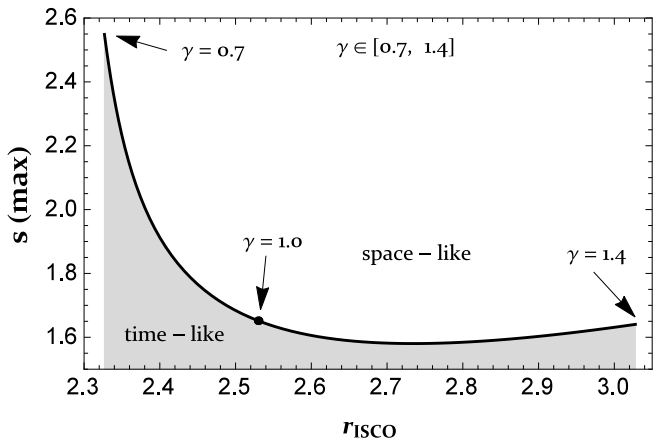


FIG. 2. Maximum value allowed for the spin of test particles at the ISCO in the  $\gamma$ -metric as a function of  $\gamma \in [0.7, 1.4]$ . The solid line separates timelike motion,  $u^\alpha u_\alpha < 0$ , from the spacelike,  $u^\alpha u_\alpha > 0$ .

TABLE I. ISCO parameters for spinning test particles with the super-luminal bound ( $u^\alpha u_\alpha = 0$ ) in the  $\gamma$ -metric.

$\gamma$	$s(\max)$	$r_{\text{ISCO}}(\min)$	$E_{\text{ISCO}}$	$L_{\text{ISCO}}$	$\Omega_{\text{ISCO}}$
1.4	1.6405	3.0278	0.8928	3.4095	0.1318
1.3	1.6019	2.8963	0.8740	2.9298	0.1411
1.2	1.5814	2.7678	0.8511	2.4271	0.1520
1.1	1.5906	2.6444	0.8231	1.8943	0.1650
1.0	1.6518	2.5299	0.7894	1.3226	0.1809
0.9	1.8083	2.4320	0.7511	0.7093	0.2009
0.8	2.1146	2.3634	0.7155	0.0962	0.2253
0.7	2.5487	2.3269	0.6946	-0.3963	0.2503

radius  $r_{\text{ISCO}} \approx 2.74$  which correspond to  $\gamma \approx 1.17$ . After that value, the superluminal limit of the spin of particle increases slowly with increasing the value of  $\gamma$ .

Of course, one can also calculate the ISCO for spinning particles in the  $\gamma$ -metric for the values of the spin parameter that do not exceed the super-luminal limit. In Fig. 3 we show the dependence of the ISCO radius of the spinning test particle located on the equatorial plane in the  $\gamma$ -metric on the three possible shapes: oblate (i.e.  $\gamma > 1$ ), spherical (i.e.  $\gamma = 1$ ), and prolate (i.e.  $\gamma < 1$ ). Fig. 4 shows the dependence of energy, angular momentum and radius of the ISCO on the value of the spin parameter, for prolate (left panel), spherical (central panel) and oblate (right panel) geometries. One more important quantity related to circular motion of a test particle is the particle's angular velocity or orbital frequency. In general, the orbital frequency of a test particle, relative to an observer at infinity is defined by  $\Omega = u^\phi/u^t$ . Then,  $\Omega_{\text{ISCO}}$  in Tabs. I and II identifies the value of the angular velocity of the particle at the ISCO. Finally, Tab. II shows the numerical values of the above quantities for different values of  $s$  and  $\gamma$ . One can easily notice that, similarly to the case of non-spinning particles, for a fixed value of  $s$ , oblateness ( $\gamma > 1$ ) implies a larger ISCO radius with respect to prolateness ( $\gamma < 1$ ).

Depending on the signs of the spin  $s$  and angular momen-

TABLE II. Characteristic parameters of ISCO of the spinning particle moving in the  $\gamma$  space-time. Where the values corresponding to  $\gamma = 1.0$  represents the ones of the Schwarzschild space-time.

$s$	$\gamma$	$r_{\text{ISCO}}$	$E_{\text{ISCO}}$	$L_{\text{ISCO}}$	$\Omega_{\text{ISCO}}$	$u_{\text{ISCO}}^2$
-0.2	1.2	7.4040	0.9460	4.0794	0.0767	-0.5224
	1.1	6.8600	0.9459	3.7224	0.0846	-0.5208
	1.0	6.3114	0.9457	3.3645	0.0945	-0.5185
	0.9	5.7562	0.9455	3.0052	0.1072	-0.5152
-0.1	0.8	5.1911	0.9450	2.6438	0.1245	-0.5102
	1.2	7.2501	0.9448	4.1305	0.0771	-0.5150
	1.1	6.7070	0.9446	3.7735	0.0851	-0.5128
	1.0	6.1594	0.9443	3.4156	0.0952	-0.5097
0.0	0.9	5.6053	0.9439	3.0562	0.1081	-0.5053
	0.8	5.0415	0.9432	2.6946	0.1257	-0.4986
	1.2	7.0900	0.9436	4.1794	0.0788	-0.5000
	1.1	6.5472	0.9433	3.8223	0.0860	-0.5000
0.1	1.0	6.0000	0.9428	3.4641	0.0962	-0.5000
	0.9	5.4464	0.9422	3.1043	0.1095	-0.5000
	0.8	4.8832	0.9412	2.7422	0.1278	-0.5000
	1.2	6.9230	0.9422	4.2260	0.0805	-0.4984
0.2	1.1	6.3800	0.9418	3.8685	0.0893	-0.4945
	1.0	5.8325	0.9411	3.5097	0.1004	-0.4892
	0.9	5.2787	0.9402	3.1492	0.1150	-0.4820
	0.8	4.7153	0.9389	2.7859	0.1352	-0.4715
0.2	1.2	6.7485	0.9408	4.2700	0.0836	-0.4892
	1.1	6.2046	0.9401	3.9118	0.0931	-0.4840
	1.0	5.6562	0.9392	3.5521	0.1052	-0.4772
	0.9	5.1013	0.9380	3.1902	0.1213	-0.4682
0.8	4.5368	0.9363	2.8252	0.1440	-0.4554	

tum  $L$  of the test particles, since the value of the ISCO depends on  $s_0 L_0$ , one can see from Fig. 3 two situations are possible, as following:

- (i) Spinning particles with spin  $s_0 > 0$  moving clockwise  $L_0 > 0$  have the same ISCO as the ones with spin  $s_0 < 0$  moving counter-clockwise  $L_0 < 0$ .
- (ii) Spinning particles with spin  $s_0 < 0$  moving clockwise  $L_0 > 0$  have the same ISCO as the ones with spin  $s_0 > 0$  moving counter-clockwise  $L_0 < 0$ .

Also, from Fig. 3 and Tab. II we see that, for fixed values of  $|s|$  and  $|L|$ , we have  $r_{\text{ISCO}}(s_0 L_0 < 0) > r_{\text{ISCO}}(s_0 L_0 > 0)$ .

From Tab. II, and similarly to what was shown in previous papers [42, 43], we see that the oblate  $\gamma$  space-time has larger ISCO radius with respect to the spherical and prolate case for non spinning test particles. However, if the test particle is spinning, the above statement is not always correct. In some cases, depending on the values of spin and angular momentum of the particle, the prolate  $\gamma$ -metric might have a larger ISCO radius than the corresponding oblate geometry. In particular, counter-spinning particles (i.e.  $s_0 L_0 < 0$ ) in the prolate geometry may have larger ISCO than co-spinning (i.e.  $s_0 L_0 > 0$ ) particles in the oblate geometry. This may be relevant when it comes to the determination of the geometry around astrophysical massive compact objects, as spinning particles in the accretion disk may make a black hole mimicker look like a black hole.



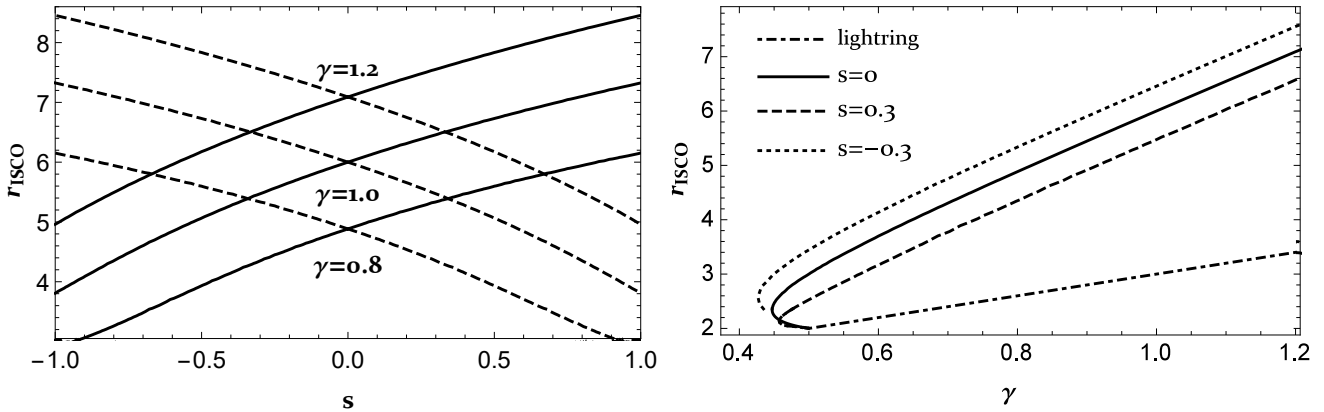


FIG. 3. Left panel: Dependence of the ISCO of spinning test particles on the equatorial plane of the  $\gamma$ -metric on the particle's spin for different values of  $\gamma$ . From upper to lower crossed lines correspond to the cases of  $\gamma = 1.2$ ,  $\gamma = 1.0$  (Schwarzschild), and  $\gamma = 0.8$ , respectively. Dashed and solid lines represent  $L_{\text{ISCO}} > 0$  and  $L_{\text{ISCO}} < 0$  cases, respectively. Right panel: Dependence of the ISCO radius on the deformation parameter  $\gamma$  for different values of the particle's spin. For completeness we illustrate also the limiting orbit give by the photon capture radius (dot-dashed line).

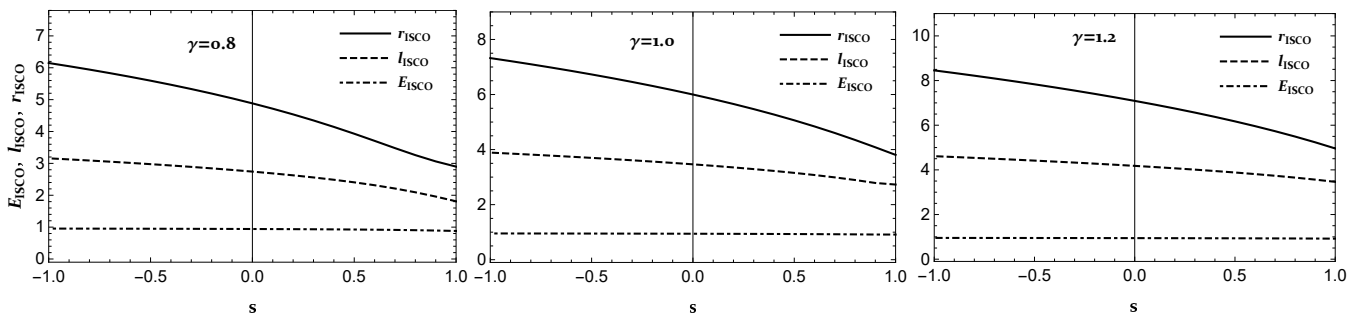


FIG. 4. Spin dependence of characteristic parameters of the test particle at the ISCO, namely energy  $E_{\text{ISCO}}$  (dot-dashed line), total angular momentum  $l_{\text{ISCO}} = L_{\text{ISCO}} + s$  (dashed line), and radius of ISCO  $r_{\text{ISCO}}$  (solid line) in the  $\gamma$ -metric. Left panel for prolate, central panel for spherical and right panel for oblate sources. The intersecting vertical line corresponds to the non-spinning particle.

#### IV. CONCLUSION

In this paper we studied the motion of spinning particles in the equatorial plane of the  $\gamma$ -metric, in the “pole-dipole” approximation by using the MPD equations with Tulczyjew-SSC. The study of the ISCO location depending on the properties of the particles in accretion disks is important in astrophysics as it is the first step towards the possibility of determining the nature of the geometry around compact objects. In our previous paper [43] we had shown the relation of the ISCO radius of neutral non-spinning test particles to the deformation parameter of the  $\gamma$ -metric. The ISCO is bigger than Schwarzschild's for oblate sources and smaller for prolate sources, namely

$$r_{\text{ISCO}}(\gamma > 1) > r_{\text{ISCO}}(\gamma = 1) \equiv 6M > r_{\text{ISCO}}(\gamma < 1). \quad (45)$$

However, in the case of a spinning test particle, the relation (45) changes depending on the spin of the particle. Therefore the most significant way to classify the orbits is in terms of the spin-angular momentum ( $s - L$ ) orientation of the par-

ticule. In Fig. 3 we showed that

$$r_{\text{ISCO}}(s_0 L_0 < 0) > r_{\text{ISCO}}(s = 0) > r_{\text{ISCO}}(s_0 L_0 > 0). \quad (46)$$

As it was mentioned above, the kinematical 4-velocity and dynamical 4-momentum of the spinning particle are not always parallel. Therefore, despite the fact that the normalization of the 4-momentum always hold, the kinematical 4-velocity may exceed the speed of light, which is not physical. Therefore, one must impose an extra condition to ensure that the particle's motion is always time-like. As a consequence of this we have shown that the allowed spin of particles located on the ISCO of  $\gamma$ -metric can be higher for prolate sources with respect to oblate sources.

The final aim is to compare the theoretical predictions for accretion disks around black holes and black hole mimickers. In this view, it is important to compare the results obtained for the  $\gamma$ -metric with the corresponding situation in the Kerr geometry. In [22, 24, 26, 27] it was shown that the value of the ISCO for spinning particles in the Kerr space-time has a wider range with respect to the case of the spinless particles. However, the lower limit of the ISCO, i.e.  $r_{\text{ISCO}} \geq M$ , re-

mains unchanged by the introduction of the spin of test particles. Similarly, here we have shown that the value of the ISCO for spinning particles in the  $\gamma$ -metric also has a wider range with respect to the case of the spinless particles. However, the lower limit of the value of the ISCO radius must remain larger than singular surface,  $r_{\text{ISCO}} > 2M$ , for small departures from spherical symmetry. Therefore, if the mass of the compact object is measured through a different method, the observation of an ISCO radius  $r_{\text{ISCO}} > 2M$  alone would not allow to determine if the central object is described by the Kerr geometry or a black hole mimicker with non vanishing quadrupole moment.

## ACKNOWLEDGMENTS

The work was developed under the Nazarbayev University Faculty Development Competitive Research Grant No. 090118FD5348. The authors acknowledge the support of the Ministry of Education of Kazakhstan's target program IRN: BR05236454 and Uzbekistan Ministry for Innovation Development Grants No. VA-FA-F-2-008 and No. YFA-Ftech-2018-8.

- 
- [1] F. de Felice, *Nuovo Cimento B Serie* **57**, 351 (1968).  
 [2] J. M. Bardeen, W. H. Press, and S. A. Teukolsky, *Astrophys. J.* **178**, 347 (1972).  
 [3] D. Pugliese, H. Quevedo, and R. Ruffini, *Phys. Rev. D* **84**, 044030 (2011), arXiv:1105.2959 [gr-qc].  
 [4] A. N. Chowdhury, M. Patil, D. Malafarina, and P. S. Joshi, *Phys. Rev. D* **85**, 104031 (2012), arXiv:1112.2522 [gr-qc].  
 [5] B. Carter, *Phys. Rev.* **174**, 1559 (1968).  
 [6] The LIGO Scientific Collaboration and the Virgo Collaboration, *Phys. Rev. Lett.* **116**, 061102 (2016), arXiv:1602.03837 [gr-qc].  
 [7] The LIGO Scientific Collaboration and the Virgo Collaboration, *Phys. Rev. Lett.* **119**, 161101 (2017), arXiv:1710.05832 [gr-qc].  
 [8] E. Barausse, E. Racine, and A. Buonanno, *Phys. Rev. D* **80**, 104025 (2009), arXiv:0907.4745 [gr-qc].  
 [9] J. Steinhoff and D. Puetzfeld, *Phys. Rev. D* **86**, 044033 (2012), arXiv:1205.3926 [gr-qc].  
 [10] E. Harms, G. Lukes-Gerakopoulos, S. Bernuzzi, and A. Nagar, *Phys. Rev. D* **94**, 104010 (2016), arXiv:1609.00356 [gr-qc].  
 [11] G. Lukes-Gerakopoulos, J. Seyrich, and D. Kunst, *Phys. Rev. D* **90**, 104019 (2014), arXiv:1409.4314 [gr-qc].  
 [12] J. Steinhoff and D. Puetzfeld, *Phys. Rev. D* **81**, 044019 (2010), arXiv:0909.3756 [gr-qc].  
 [13] M. Mathisson, *Acta Phys. Pol.* **6**, 163 (1937).  
 [14] A. Papapetrou, *Proc. R. Soc. A* **209**, 248 (1951).  
 [15] W. G. Dixon, *Proc. R. Soc. A* **314**, 499 (1970).  
 [16] W. G. Ramirez and A. A. Deriglazov, *Phys. Rev. D* **96**, 124013 (2017), arXiv:1709.06894 [gr-qc].  
 [17] A. A. Deriglazov and W. G. Ramirez, *Adv. Math. Phys.* **2017**, 7397159 (2017), arXiv:1710.07135 [gr-qc].  
 [18] W. Tulczyjew, *Acta Phys. Pol.* **18**, 393 (1959).  
 [19] F. A. E. Pirani, *Acta Phys. Pol.* **15**, 389 (1956).  
 [20] R. Hojman and S. Hojman, *Phys. Rev. D* **15**, 2724 (1977).  
 [21] M. A. Abramowicz and M. Calvani, *MNRAS* **189**, 621 (1979).  
 [22] S. Suzuki and K.-I. Maeda, *Phys. Rev. D* **58**, 023005 (1998), arXiv:gr-qc/9712095 [gr-qc].  
 [23] Z. Stuchlík, *Acta Phys. Slovaca* **49**, 319 (1999).  
 [24] O. Semerák, *MNRAS* **308**, 863 (1999).  
 [25] Z. Stuchlík and J. Kovár, *Classical and Quantum Gravity* **23**, 3935 (2006), arXiv:gr-qc/0611153 [gr-qc].  
 [26] K. Kyrian and O. Semerák, *MNRAS* **382**, 1922 (2007).  
 [27] R. Plyatsko and M. Fenyk, *Phys. Rev. D* **87**, 044019 (2013), arXiv:1303.4707 [gr-qc].  
 [28] W.-B. Han, *Gen. Rel. Grav.* **40**, 1831 (2008), arXiv:1006.2229 [gr-qc].  
 [29] W.-B. Han, *Phys. Rev. D* **82**, 084013 (2010), arXiv:1008.3324 [gr-qc].  
 [30] E. Hackmann, C. Lämmerzahl, Y. N. Obukhov, D. Puetzfeld, and I. Schaffer, *Phys. Rev. D* **90**, 064035 (2014), arXiv:1408.1773 [gr-qc].  
 [31] P. I. Jefremov, O. Y. Tsupko, and G. S. Bisnovatyi-Kogan, *Phys. Rev. D* **91**, 124030 (2015), arXiv:1503.07060 [gr-qc].  
 [32] Y.-P. Zhang, S.-W. Wei, W.-D. Guo, T.-T. Sui, and Y.-X. Liu, *Phys. Rev. D* **97**, 084056 (2018), arXiv:1711.09361 [gr-qc].  
 [33] D. M. Zipoy, *J. Math. Phys.* **7**, 1137 (1966).  
 [34] B. H. Voorhees, *Phys. Rev. D* **2**, 2119 (1970).  
 [35] D. Papadopoulos, B. Stewart, and L. Witten, *Phys. Rev. D* **24**, 320 (1981).  
 [36] W. B. Bonnor, *Gen. Relativ. Gravit.* **24**, 551 (1992).  
 [37] L. Herrera, F. M. Paiva, N. O. Santos, and V. Ferrari, *Int. J. Mod. Phys. D* **9**, 649 (2000), arXiv:gr-qc/9812023 [gr-qc].  
 [38] L. Herrera, F. M. Paiva, and N. O. Santos, *J. Math. Phys.* **40**, 4064 (1999), gr-qc/9810079.  
 [39] K. Boshkayev, E. Gasperín, A. C. Gutiérrez-Piñeres, H. Quevedo, and S. Toktarbay, *Phys. Rev. D* **93**, 024024 (2016), arXiv:1509.03827 [gr-qc].  
 [40] C. A. Benavides-Gallego, A. Abdurjabbarov, D. Malafarina, B. Ahmedov, and C. Bambi, *Phys. Rev. D* **99**, 044012 (2019), arXiv:1812.04846 [gr-qc].  
 [41] J. L. Hernandez-Pastora, L. Herrera, and J. Ospino, *Phys. Rev. D* **88**, 064041 (2013), arXiv:1309.2455 [gr-qc].  
 [42] A. B. Abdikamalov, A. A. Abdurjabbarov, D. Ayzenberg, D. Malafarina, C. Bambi, and B. Ahmedov, *Phys. Rev. D* **100**, 024014 (2019), arXiv:1904.06207 [gr-qc].  
 [43] B. Toshmatov, D. Malafarina, and N. Dadhich, *Phys. Rev. D* **100**, 044001 (2019), arXiv:1905.01088 [gr-qc].  
 [44] H. P. Künzle, *J. Math. Phys.* **13**, 739 (1972).  
 [45] S. A. Hojman and F. A. Asenjo, *Classical and Quantum Gravity* **30**, 025008 (2013), arXiv:1203.5008 [physics.gen-ph].  
 [46] J. L. Hernández-Pastora and J. Martín, *Gen. Rel. Grav.* **26**, 877 (1994).  
 [47] K. S. Virbhadra, arXiv e-prints, gr-qc/9606004 (1996), arXiv:gr-qc/9606004 [astro-ph].

## Appendix A: Effective potential

For completeness, we present here the complete analytical expression for the effective potential of spinning particles in the  $\gamma$ -metric

$$\begin{aligned}
V_+ = & \left(1 - \frac{2M}{r}\right)^{(2-\gamma)(\gamma-1)/2} \left(1 - \frac{M}{r}\right)^{\gamma^2-1} \frac{sr[r - (2\gamma+1)M]}{r^4 - s^2z} \\
& + \left(1 - \frac{2M}{r}\right)^{\gamma/2} \frac{r^4 + s^2w}{r^4 - s^2z} \sqrt{\left(1 - \frac{2M}{r}\right)^{\gamma-1} \frac{L^2}{r^2} + m^2 \left(1 - \frac{s^2z}{r^4}\right)}, \tag{A1}
\end{aligned}$$

---

where

---

$$\begin{aligned}
w = & \left(1 - \frac{M}{r}\right)^{2(\gamma^2-1)} \left(1 - \frac{2M}{r}\right)^{-\gamma^2+\gamma-1} M\gamma(\gamma M + M - r), \\
z = & \left(1 - \frac{M}{r}\right)^{2(\gamma^2-1)} \left(1 - \frac{2M}{r}\right)^{-\gamma^2+\gamma-1} (\gamma M + M - r)^2.
\end{aligned}$$


---